All-optical discrete vortex switch

Anton S. Desyatnikov,[1] Mark R. Dennis,[2] and Albert Ferrando[3]

[1]*Nonlinear Physics Center, Research School of Physics and Engineering, The Australian National University, Canberra, ACT 0200, Australia*

[2]*H. H. Wills Physics Laboratory, University of Bristol, Tyndall Avenue, Bristol BS8 1TL, United Kingdom*

[3]*Interdisciplinary Modeling Group, InterTech and Departament d'Optica, Universitat de Valéncia, E-46100 Burjassot, Spain*

(Received 28 August 2010; published 20 June 2011)

We introduce discrete vortex solitons and vortex breathers in circular arrays of nonlinear waveguides. The simplest vortex breather in a four-waveguide coupler is a nonlinear dynamic state changing its topological charge between $+1$ and -1 periodically during propagation. We find the stability domain for this solution and suggest an all-optical vortex switching scheme.

DOI: 10.1103/PhysRevA.83.063822 PACS number(s): 42.65.Tg, 42.65.Hw, 42.65.Pc

I. INTRODUCTION

Topological quantities, by their discrete nature, are well-suited for noise-free information transfer and processing. An important example is the topological charge (TC) of a quantized vortex, i.e., the integer phase change, in units of 2π, around a node in a complex scalar wave function [1]. Quantized vortices are familiar in optical [2] and matter waves [3], with applications including many-level quantum entanglement [4], quantum information storage [5], and free-space optical information transfer [6]. In order to operate with TC as an information carrier, however, it is necessary to be able to switch it from one discrete value to another.

The circulation of vortex energy is associated with orbital angular momentum, which is conserved in rotation-invariant media. Therefore, TC switching requires a vortex to exchange momentum, for example, with the underlying nonlinear periodic lattice [7], where vortices exist in the form of discrete vortex solitons [8]. Since vortices are essentially two-dimensional objects, the majority of recent work considered discrete vortex solitons in two-dimensional periodic nonlinear media, including square [7–14], triangular [15–17], and quasiperiodic [18] lattices, realized experimentally in photorefractive crystals [11,12,16,17]. More generally, discrete vortices can be defined on any closed contour of several sites, including extended states on square [13,14] or ring-like [18–21] configurations. The simplest (quasi-one-dimensional) system for studying discrete vortices is a circular array of coupled waveguides [21–23], similar to discretized vortex solitons in bulk media [24]. Until now, however, no systematic study on the existence and stability of ring-like discrete vortex solitons has been reported.

Purely discrete systems [25–27] provide the most general framework for studying networks of nonlinear coupled oscillators, and the circulation of the power flow between occupied sites identifies the presence of a discrete vortex. The "charge flipping" of discrete vortices [7,12–14] reveals itself as a reversal of the direction of the current [9,13]. At the same time, the optical vortices in continuous fields correspond to phase singularities, forming continuous lines. The charge flipping involves topological reactions between several vortex lines [12,16,28], such as hyperbolic avoided crossings [2,29]. An important question for TC control is whether the discrete analog of a continuous field retains enough information to recover the topology of the supermode and the trajectories of quantized vortices, without additional assumptions on the specific mode profile at each site [21].

Here we introduce discrete vortex solitons in circular arrays of coupled nonlinear waveguides. We solve analytically the corresponding linear stability problem and analyze the nonlinear dynamics numerically. A method to reconstruct continuous phase profile of the supermode is developed, which allows tracing of the spatial trajectories of individual phase dislocations. We obtain discrete vortex breathers with periodic inversion of TC and identify the stability domain of the breather in a four-waveguide coupler. The frequency of charge flipping is proportional to the total optical power in the waveguides and, in a coupler of fixed length, the output TC of a stable breather is fully controlled by the input power.

II. MODEL AND SOLITON SOLUTIONS

We begin with the discrete nonlinear Schrödinger equation governing the propagation of light in weakly coupled waveguides with Kerr nonlinearity [25,26]:

$$i\,\partial_z E_n + E_{n-1} + E_{n+1} + \delta|E_n|^2 E_n = 0, \quad n = 1 \ldots N, \quad (1)$$

where $\delta = +1$ for focusing and $\delta = -1$ for defocusing nonlinearities, N is the number of waveguides in the ring, and periodicity requires $E_{n+N} = E_n$; see Fig. 1(a).

For an infinite planar array of waveguides, $N \to \infty$, the so-called continuous limit can be applied, recovering the completely integrable nonlinear Schrödinger equation [25,26]. For self-focusing nonlinearity with $\delta = 1$ the localized bright solitons can be obtained, including moving solitons. Their discrete analog was studied as a possible "soliton switch," i.e., a localized wave traveling along a circular array and thereby switching the signal between different waveguides [22]. For a small number of waveguides, however, such localized excitation can lead to irregular and chaotic dynamics, such as the case of $N = 3, 4$ studied in Ref. [25]. On the other hand, the simplest nonlinear solution with a nonvanishing current is a plane wave, $E_n = A\exp(in\Theta + ikz)$, with A the (real) amplitude, k the wave number, and Θ a continuous variable which determines the internal power flow from the nth waveguide, $J_n \equiv 2\,\mathrm{Im}(E_n^* E_{n+1}) = 2A^2 \sin\Theta$.

For a circular array of coupled waveguides in Eq. (1), the periodicity requires $\exp(iN\Theta) = 1$, and thus Θ is quantized,

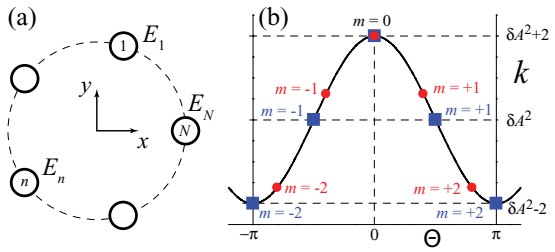

FIG. 1. (Color online) (a) Scheme for the circular array of nonlinear waveguides. (b) Dispersion relation Eq. (2) visualized for $N = 4$ (blue squares) and $N = 5$ (red circles). Vertical lines show the edges of the first Brillouin zone, $|\Theta| \leqslant \pi$.

$\Theta \to \Theta_m \equiv 2\pi m/N$, with an integer index m which we associate with the TC of the discrete vortex. The corresponding discrete vortex soliton solutions are given by

$$k = \delta A^2 + 2\cos\Theta_m, \tag{2}$$

which is plotted in Fig. 1(b). It reproduces the sketch of the angular Bloch-wave spectrum derived from symmetry considerations in Ref. [30]. Because the first Brillouin zone is limited by the values $|\Theta_m| \leqslant \pi$, the TC is limited from above [19,20], $|m| \leqslant N/2$, and staggered (multipole) modes appear for even $N = 2|m|$ at the zone edges. The TC for any set of complex numbers $\{E_n\}$ on a ring is defined as

$$m = \frac{1}{2\pi}\sum \arg(E_n^* E_{n+1}), \tag{3}$$

with the argument taking the values $\arg(\zeta) \in [-\pi,\pi]$.

III. STABILITY OF DISCRETE VORTEX SOLITONS

To study the stability of these vortex solitons, we introduce a small perturbation to each waveguide, $E_n = (A + p_n)\exp(in\Theta_m + ikz)$. The exponentially growing perturbation is $p_n = u_n\exp(\lambda z) + v_n^*\exp(\lambda^* z)$, where λ is an eigenvalue of the linear stability problem for the modes u_n and v_n:

$$\begin{aligned} -i\lambda u_n &= Bu_n + \delta A^2 v_n + u_{n-1}e^{-i\Theta_m} + u_{n+1}e^{i\Theta_m}, \\ i\lambda v_n &= Bv_n + \delta A^2 u_n + v_{n-1}e^{i\Theta_m} + v_{n+1}e^{-i\Theta_m}, \end{aligned} \tag{4}$$

with $B = \delta A^2 - 2\cos\Theta_m$ and the solution is linearly unstable if $\mathrm{Re}(\lambda) > 0$. Applying the ring periodicity to the perturbation modes, $u_{n+N} = u_n$ and $v_{n+N} = v_n$, allows one to solve Eqs. (4) using the discrete Fourier transform, $u_n = \sum_s U_s\exp(in\Theta_s)$ and $v_n = \sum_s V_s\exp(in\Theta_s)$. The eigenvalues λ_s of the mode $\{U_s, V_s\}$ are given by

$$\begin{aligned} \lambda_s &= -i2\sin\Theta_m\sin\Theta_s \pm i2\sin(\Theta_s/2)\sqrt{D}, \\ D &= 2\cos\Theta_m[2\cos\Theta_m\sin^2(\Theta_s/2) - \delta A^2], \end{aligned} \tag{5}$$

so that the solution is linearly stable if $D \geqslant 0$ for all possible $|s| \leqslant N/2$, and unstable otherwise. Note that all solutions are stable for $N = 4|m|$ as well as in the linear limit, $A \to 0$. Therefore, the instabilities can only appear for some supercritical amplitude, $A > A_{\mathrm{stab}}$.

We illustrate the stability of discrete vortex solitons for the case $N = 6$, similar to continuous systems with sixfold rotational symmetry, such as hexagonal photonic lattices [17] and Bessel potentials [20]. A corresponding discrete system was studied earlier [31] as a model for hexagonal benzene molecule, and different vibrational modes were identified, including vortex solutions. In accordance with Eq. (2), there are four vortex solitons with $|m| = 1,2$, one plane wave with $m = 0$, and one staggered mode with $|m| = 3$. Of particular interest is the inverse stability of vortices in focusing media: while the lowest-order vortex solitons with $|m| = 1$ become unstable for $A > A_{\mathrm{stab}} = 1/2$, the double-charge solitons with $|m| = 2$ are stable for any A. The results of numerical integration of Eq. (1) in Fig. 2 confirm these predictions.

The dynamics of the TC for the unstable single-charged vortex in Fig. 2(a) is strongly irregular, spanning all available values $-2 \leqslant m \leqslant 2$. An important question here is whether such dynamics has a continuous analog with nucleating phase singularities. To reveal the topological picture of discrete vortex dynamics, we construct a continuous interpolating complex function (optical field of the supermode) $E(x,y)$, which takes the value of the field in the nth waveguide, $E_n = E(x_n,y_n)$, at its spatial location, $x_n + iy_n = r_0\exp(i\Theta_n)$, where $r_0 = 1$ is the radius of the array. We devise such a natural affine linear map as a set of linear transformations, stitched together along vertices of the angular segments $\varphi \in [\Theta_n,\Theta_{n+1})$, where

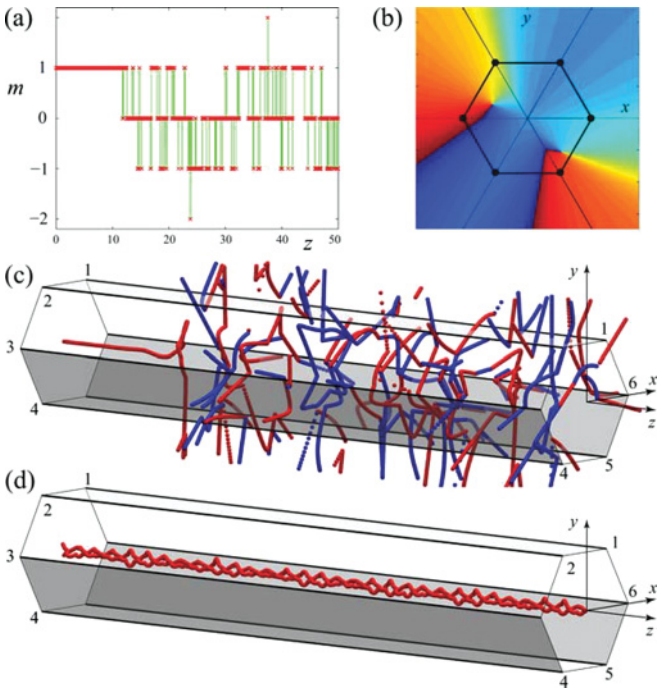

FIG. 2. (Color online) (a) Unstable dynamics of a discrete vortex with TC $m = 1$ in an array of $N = 6$ waveguides with self-focusing nonlinearity. (b) The discrete-to-continuous map Eq. (6) of phase $\arg E$ at $z = 32.3$: while the charge in (a) is zero at this point, the map in (b) shows two vortices of opposite charges inside the hexagon. (c) The trajectories of interpolated vortices (red with $m = +1$ and blue with $m = -1$) for solution in (a). (d) Stable dynamics of a double-charge vortex, $m = 2$, with two single-charge vortices spiraling about the optical axis. In both cases $A = 1$ while the initial perturbation is 0.01% in (a–c) and 20% in (d).

$x + iy = r\exp(i\varphi)$. We obtain $E(r,\varphi) = \bar{E} + r\Psi_n(\varphi)/\sin(\Theta_1)$ with the arithmetic mean $\bar{E} = \frac{1}{N}\sum_n E_n$ and

$$\Psi_n(\Theta_n \leqslant \varphi < \Theta_{n+1}) = (E_{n+1} - \bar{E})\sin(\varphi - \Theta_n) - (E_n - \bar{E})\sin(\varphi - \Theta_{n+1}). \quad (6)$$

Geometrically, the field inside each triangle with vertices $0,(r_0,\Theta_n),(r_0,\Theta_{n+1})$ is a linear image of the region of the complex plane enclosed by the triangle $\bar{E},E_n,E_{n+1}$, and it cannot carry more than one phase singularity.

An example of the continuous phase profile in Fig. 2(b) is derived for the solution in Fig. 2(a) at the particular propagation length $z = 32.2$, and it provides important information about this state, otherwise hidden. Indeed, the TC is zero, which might indicate the absence of vortices, while in reality the topology of the supermode is more complex, with two phase singularities of opposite charge inside a hexagon. Furthermore, the map Eq. (6) endows each vortex with a position coordinate, through the solution of $E(r,\varphi) = 0$ at each propagation step z, the results for an unstable solution are plotted in Fig. 2(c). Clearly, as the instability develops, there are many vortices inside and outside the hexagon, while the TC in Fig. 2(a) only accounts for the total charge of all vortices inside the hexagon. This picture is in sharp contrast with the stable double-charge solution in Fig. 2(d); in fact, a very large initial perturbation was necessary for two elementary vortices to split and spiral about the origin.

IV. VORTEX BREATHERS

Our method allows the detailed study of the dynamics of vortex breathers. Charge-flipping breather solutions to Eq. (1) in a chain of $N = 4l$ sites ($l = 1,2,\ldots$) can be introduced [23] with two decoupled staggered sublattices,

$$E_{2j-1} = (-1)^j a\exp(i\delta a^2 z + i\alpha),$$
$$E_{2j} = (-1)^j b\exp(i\delta b^2 z + i\beta), \quad (7)$$

where $j = 1,\ldots,2l$ and the amplitudes a, b and phases α, β are arbitrary. According to Eq. (3), the TC, $m = \sigma l$, changes periodically with propagation, $\sigma = -\mathrm{sgn}(\sin\omega\tilde{z})$, where $\tilde{z} = z + (\alpha - \beta)/\omega$ and the frequency of charge-flipping $\omega = \delta(a^2 - b^2)$. This solution is symmetric with respect to the simultaneous inversion $\delta \to -\delta$ and complex conjugation, thus its stability does not depend on the type of nonlinearity, focusing or defocusing.

The stability of the breather solution with two frequencies, $\omega_a = \delta a^2$ and $\omega_b = \delta b^2$, is studied numerically using Floquet analysis [9]. We focus here on the lowest-order case of four waveguides, $N = 4$ and $m = \pm 1$, also choosing $\delta = 1$ and $\omega_a \geqslant \omega_b$ without loss of generality. The corresponding symplectic Floquet matrix has $2N$ eigenvalues Λ_j which, for stable solutions, must all lie on a unit circle, $|\Lambda_j| = 1$. We thus introduce a stability parameter, $\bar{\Lambda} = ||\Lambda_j||/\sqrt{2N}$, to distinguish between stable ($\bar{\Lambda} = 1$) and unstable ($\bar{\Lambda} > 1$) solutions. The stability diagram $\bar{\Lambda}(\omega_a,\omega_b)$ in Fig. 3(a) is conveniently represented in the domain of two parameters: the power $P \equiv \sum_n |E_n|^2 = 2(\omega_a + \omega_b)$ and the frequency ratio $\eta = \omega_b/\omega_a$. The region $\omega < 0.02$ in Fig. 3(a) is not explored because finding numerical solutions is increasingly difficult

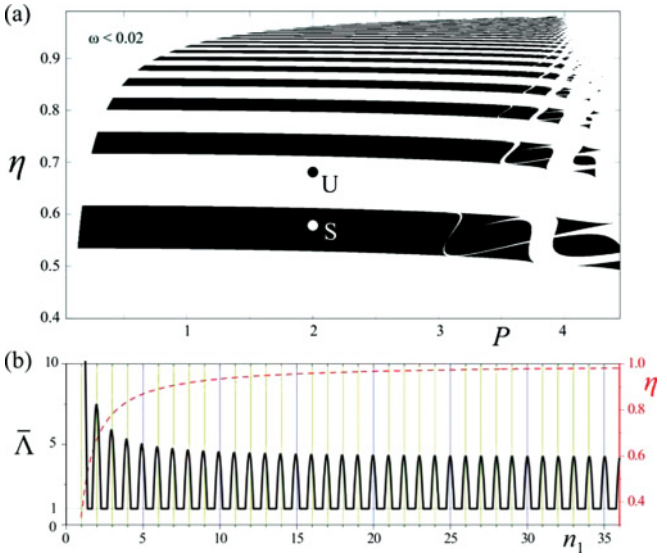

FIG. 3. (Color online) (a) Stability diagram of the vortex breather in $N = 4$ coupled Kerr waveguides; the stability islands with $\bar{\Lambda} = 1$ are shaded dark grey, the light grey top left corner with $\omega < 0.02$ is unexplored. The dots mark stable (S) and unstable (U) solutions explored in Fig. 4. (b) A cross section at $P = 2$ of the diagram in (a); the red dashed line helps the eye to map n_1 to η (right axis).

as the periods $T = 2\pi/\omega$ diverge. Nevertheless, in the linear limit, $P \to 0$, we do not expect any instability to appear, while in the limit $\eta = 1$ and $a = b = A$, this solution recovers unconditionally stable vortex solitons with $m = \pm l$, $\alpha = \mp\pi/2$, and $\beta = 0$. For small differences, $|a - b| \ll (a + b)$, a breather solution can be described as a stable vortex soliton perturbed by modes with $\lambda_{\pm 2l} = 0$, in agreement with the limit

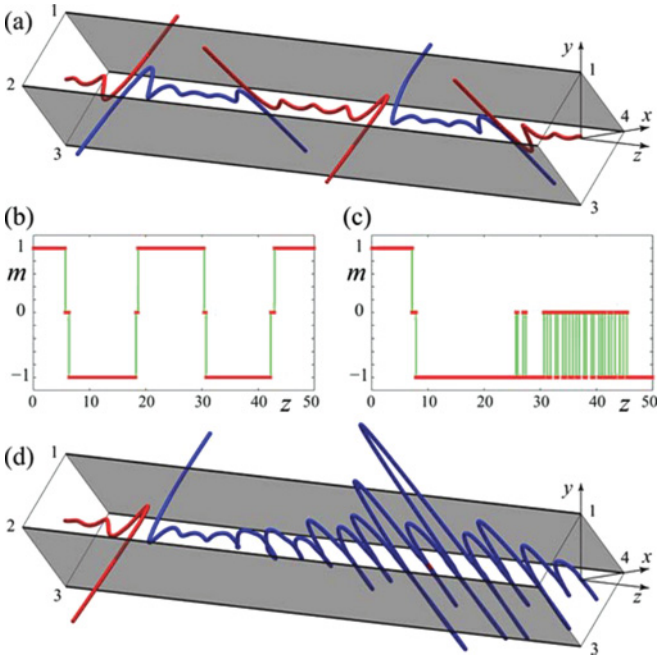

FIG. 4. (Color online) (a, b) Regular charge flipping of the perturbed stable breather with $\eta = 0.58$ and (c, d) irregular dynamics of unstable breather with $\eta = 0.67$; in both cases $P = 2$ as marked by dots in Fig. 3(a).

$\omega \to 0$ for $\eta \to 1$. However, close to this limit in Fig. 3(a), we observe the appearance of many narrow instability bands. Their positions became almost regularly aligned with integer n_1 in Fig. 3(b), where $n_1 = n_0/(1-\eta)$ with fitting parameter $n_0 = 0.655$, similar to the instability condition $n_0 = 2$ for the two-site breather in square lattices [9].

We aim to establish the possibility of a robust control over the TC of the vortex breather. The first stability band [the lowest dark-shaded stripe in Fig. 3(a)] provides an optimal parameter domain because it corresponds to the shortest available periods T. Figure 4 illustrates the continuous line trajectories of the interpolated optical vortices carried by stable (a) and unstable (d) breathers. In the former case with $\eta = 0.58$, the periodic charge flipping in Fig. 4(b) appears in (a) as a series of near-reconnection events with sharp turns in the vortex trajectories [32]. In contrast, the unstable solution with $\eta = 0.67$ develops irregular dynamics, with TC in Fig. 4(c) oscillating between -1 and zero as the vortex line in (d) is moving in and out of the square with four waveguides at its corners.

The stable vortex breather in Figs. 4(a) and 4(b) can be used as an all-optical switch of the output TC versus input power P. To realize that, an optical mask at the input can be employed, transforming signal with power P into a discrete vortex with charge $m = +1$ and modulation depth $\eta = 0.58$ in the first stable band. For waveguides of fixed length L, the power acts as the charge-flipping parameter, $m = \mathrm{sgn}(\cos P\tilde{L})$, with $\tilde{L} = \frac{L}{2}\frac{1-\eta}{1+\eta} = 0.133L$. TC switch occurs at the output whenever the input power changes by $\pi/\tilde{L}$. With increase of power up to $P = 3$ along the horizontal line $\eta = 0.58$ through the S point in Fig. 3(a), the output TC switches once for $L = 10$, while for $L = 100$ the input signal (power) is discriminated into a series of 12 alternating output values $m = \pm 1$.

V. CONCLUSIONS

In conclusion, we have introduced discrete vortex solitons and breathers in circular arrays of coupled nonlinear waveguides. We identified the soliton stability domains and developed a numerical method to recover the topology of interpolated phase singularities, which explains and illustrates the physical mechanism of discrete vortex dynamics. A robust scheme for all-optical control over the topological charge of a discrete vortex is suggested using a stable vortex breather in a four-waveguide coupler.

ACKNOWLEDGMENTS

This work is supported by the Australian Research Council, the Royal Society of London, and by the Government of Spain under Contracts No. TIN2006-12890 and TEC2010-15327. Authors thank J. H. Hannay and Yu. S. Kivshar for useful discussions.

[1] J. F. Nye and M. V. Berry, Proc. R. Soc. London A **336**, 165 (1974).

[2] M. S. Soskin and M. V. Vasnetsov, *Progress in Optics*, edited by E. Wolf, Vol. 42 (Elsevier, Amsterdam, 2001), p. 219; M. R. Dennis, K. O'Holleran, and M. J. Padgett, Prog. Opt. **52**, 293 (2009).

[3] J. E. Williams and M. J. Holland, Nature **401**, 568 (1999); M. R. Matthews, B. P. Anderson, P. C. Haljan, D. S. Hall, C. E. Wieman, and E. A. Cornell, Phys. Rev. Lett. **83**, 2498 (1999).

[4] A. Mair *et al.*, Nature **412**, 313 (2001); G. Molina-Terriza, J. P. Torres, and L. Torner, Phys. Rev. Lett. **88**, 013601 (2002).

[5] Z. Dutton and J. Ruostekoski, Phys. Rev. Lett. **93**, 193602 (2004).

[6] G. Gibson *et al.*, Opt. Express **12**, 5448 (2004).

[7] T. J. Alexander, A. A. Sukhorukov, and Yu. S. Kivshar, Phys. Rev. Lett. **93**, 063901 (2004).

[8] B. A. Malomed and P. G. Kevrekidis, Phys. Rev. E **64**, 026601 (2001).

[9] M. Johansson *et al.*, Physica D **119**, 115 (1998).

[10] J. Yang and Z. H. Musslimani, Opt. Lett. **28**, 2094 (2003); J. Yang, New J. Phys. **6**, 47 (2004).

[11] D. N. Neshev, T. J. Alexander, E. A. Ostrovskaya, Y. S. Kivshar, H. Martin, I. Makasyuk, and Z. Chen, Phys. Rev. Lett. **92**, 123903 (2004); J. W. Fleischer, G. Bartal, O. Cohen, O. Manela, M. Segev, J. Hudock, and D. N. Christodoulides, *ibid.* **92**, 123904 (2004).

[12] J. Yang, I. Makasyuk, P. G. Kevrekidis, H. Martin, B. A. Malomed, D. J. Frantzeskakis, and Z. Chen, Phys. Rev. Lett. **94**, 113902 (2005); A. Bezryadina *et al.*, Opt. Express **14**, 8317 (2006); Opt. Lett. **31**, 2456 (2006).

[13] D. E. Pelinovsky, P. G. Kevrekidis, and D. J. Frantzeskakis, Physica D **212**, 20 (2005); M. Öster and M. Johansson, Phys. Rev. E **73**, 066608 (2006).

[14] M. S. Petrović, S. Prvanović, and D. M. Jović, Phys. Rev. A **79**, 021803(R) (2009); K. J. H. Law, D. Song, P. G. Kevrekidis, J. Xu, and Z. Chen, Phys. Rev. A **80**, 063817 (2009).

[15] P. G. Kevrekidis, B. A. Malomed, and Yu. B. Gaididei, Phys. Rev. E **66**, 016609 (2002); K. J. H. Law, P. G. Kevrekidis, V. Koukouloyannis, I. Kourakis, D. J. Frantzeskakis, and A. R. Bishop, *ibid.* **78**, 066610 (2008).

[16] B. Terhalle, T. Richter, A. S. Desyatnikov, D. N. Neshev, W. Krolikowski, F. Kaiser, C. Denz, and Y. S. Kivshar *et al.*, Phys. Rev. Lett. **101**, 013903 (2008); B. Terhalle *et al.*, Opt. Lett. **35**, 604 (2010).

[17] K. J. H. Law, P. G. Kevrekidis, T. J. Alexander, W. Krolikowski, and Y. S. Kivshar, Phys. Rev. A **79**, 025801 (2009); B. Terhalle *et al.*, *ibid.* **79**, 043821 (2009).

[18] K. J. H. Law, A. Saxena, P. G. Kevrekidis, and A. R. Bishop, Phys. Rev. A **82**, 035802 (2010).

[19] A. Ferrando *et al.*, Opt. Express **12**, 817 (2004); A. Ferrando, M. Zacarés, and M.-Á. García-March, Phys. Rev. Lett. **95**, 043901 (2005).

[20] Y. V. Kartashov, A. Ferrando, A. A. Egorov, and L. Torner, Phys. Rev. Lett. **95**, 123902 (2005).

[21] C. N. Alexeyev, A. V. Volyar, and M. A. Yavorsky, Phys. Rev. A **80**, 063821 (2009).

[22] C. Schmidt-Hattenberg *et al.*, Opt. Commun. **82**, 461 (1991); **89**, 473 (1992); W. Krolikowski *et al.*, Opt. Lett. **19**, 320 (1994).

[23] L. Casetti and V. Penna, J. Low Temp. Phys. **126**, 455 (2002).

[24] M. Soljačić and M. Segev, Phys. Rev. Lett. **86**, 420 (2001); A. S. Desyatnikov and Yu. S. Kivshar, *ibid*. **88**, 053901 (2002); A. S. Desyatnikov, A. A. Sukhorukov, and Yu. S. Kivshar, *ibid.* **95**, 203904 (2005).

[25] J. C. Eilbeck, P. S. Lomdahl, and A. C. Scott, Physica D **16**, 318 (1985).

[26] D. N. Christodoulides and R. I. Joseph, Opt. Lett. **13**, 794 (1988); Yu. S. Kivshar, *ibid*. **18**, 1147 (1993).

[27] F. Lederer *et al.*, Phys. Rep. **463**, 1 (2008); S. Flach and A. V. Gorbach, *ibid*. **467**, 1 (2008).

[28] A. Ferrando, M. Zacares, M. A. Garcia-March, J. A. Monsoriu, and P. F. deCordoba, Phys. Rev. Lett. **95**, 123901 (2005); M.-Á. García-March, A. Ferrando, M. Zacares, S. Sahu, and D. E. Ceballos-Herrera, Phys. Rev. A **79**, 053820 (2009); M. Zacarés, M. A. Garcia-March, J. Vijande, A. Ferrando, and E. Merino, *ibid*. **80**, 043812 (2009).

[29] A. S. Desyatnikov, Yu. S. Kivshar, and L. Torner, in *Progress in Optics*, edited by E. Wolf, Vol. 47 (Elsevier, Amsterdam, 2005), p. 291.

[30] A. Ferrando, Phys. Rev. E **72**, 036612 (2005); M.-Á. García-March *et al.*, Physica D **238**, 1432 (2009).

[31] A. C. Scott and J. C. Eilbeck, Chem. Phys. Lett. **132**, 23 (1986); J. C. Eilbeck, in *Physics of Many-Particle Systems*, edited by A. Davydov, Vol. 12, (Kiev, Naukova Dumka, 1987), pp. 41–51.

[32] G. Molina-Terriza, J. Recolons, J. P. Torres, L. Torner, and E. M. Wright, Phys. Rev. Lett. **87**, 023902 (2001).